

Isolation and Oxidation-Reduction of Methylviologen Cation Radicals. Novel Disproportionation in Charge-Transfer Salts by X-ray Crystallography

T. M. Bockman and J. K. Kochi*

Department of Chemistry, University of Houston, Houston, Texas 77204-5641

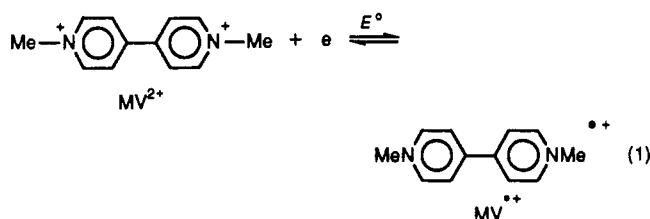
Received December 27, 1989

The totally reversible reduction of the well-known organic electron mediator methylviologen dication MV^{2+} to its cation radical $MV^{\bullet+}$ and thence to the neutral MV^0 is established by cyclic voltammetric studies in nonaqueous solutions. The use of aprotic solvents thus allows crystalline forms of $MV^{\bullet+}$ and MV^0 to be isolated and structurally characterized for the first time by X-ray crystallography. The structural parameters of MV^0 show it to be a nonaromatic, polyene-like dihydrobipyridine (similar to dipyrans and dithiopyrans) with excellent electron-donor properties. The crystalline methylviologen cation radical (as the 1:1 salt $MV^{\bullet+}PF_6^-$) exists as an infinite stack of structurally distinct cationic moieties that are designated as MVI and MVII. Structural parameters show that the MVI component is related to the oxidized MV^{2+} , and MVII is related to the reduced MV^0 . The alternate stacking of MVI and MVII in $MV^{\bullet+}PF_6^-$ is ascribed to a unique intracrystalline disproportionation that derives from strong charge-transfer interactions inherent to the methylviologen cation radical. The phenomenological relationship of such charge-transfer forces to the dimeric $(MV^{\bullet+})_2$ extant in concentrated aqueous solutions and to properties relevant to organic metals is advanced.

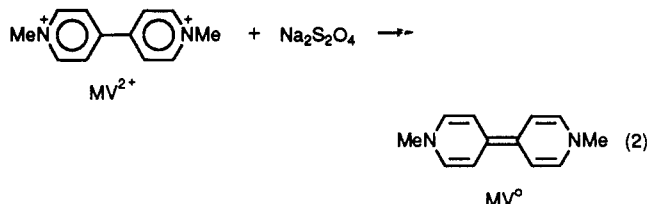
Introduction

Since the discovery of its reduction by Michaelis in 1932,¹ the bis-quaternary salt of the *N,N'*-dimethyl-4,4'-bipyridinium dication, commonly referred to as methylviologen (MV^{2+}), has been established as the prototypical electron-transfer reagent.² Indeed the principal role of MV^{2+} as the electron mediator in various types of photochemical,³⁻⁵ radiolytic,⁶ and electrochemical^{2,7} applications extends to its use as an herbicide⁸ and in water-splitting systems.^{9,10} Central to its efficacy is the facile one-electron

reduction of methylviologen to its cation radical, i.e.



at the reversible potential of $E^0 = -0.687$ V vs SCE in aqueous solutions.² However the cation radical of methylviologen is extremely sensitive to air,¹¹ and $MV^{\bullet+}$ has never been isolated as a crystalline salt. Furthermore the reduction of methylviologen in aqueous solution by chemical reducing agents such as sodium dithionite yields the neutral dihydrobipyridyl derivative MV^0 , i.e.^{12,13}



which corresponds to an overall two-electron reduction. Like the cation radical, MV^0 undergoes ready oxidation upon exposure to air. Although the reduced forms $MV^{\bullet+}$ and MV^0 have been spectrally examined in solution,¹⁴ thin films,¹⁵ and zeolites,¹⁶ the pertinent structural information

(11) Yoon, K. B.; Kochi, J. K. *J. Am. Chem. Soc.* 1988, 110, 6586 for leading references.

(12) Carey, J. G.; Cairns, J. F.; Colchester, J. E. *J. Chem. Soc., Chem. Commun.* 1969, 1280.

(13) Mohammad, M. *J. Org. Chem.* 1987, 52, 2779.

(14) (a) Rieger, A. L.; Edwards, J. O. *J. Org. Chem.* 1988, 53, 1481. (b) Summers, L. A. *Adv. Heterocycl. Chem.* 1984, 35, 281. (c) Novakovic, Y.; Hoffman, M. Z. *J. Am. Chem. Soc.* 1987, 109, 2341.

(15) (a) Widrig, C. A.; Majda, M. *Langmuir* 1989, 5, 689. (b) Wolszczak, M.; Stradowski, C. *Radiat. Phys. Chem.* 1989, 33, 355. (c) Lee, C. W.; Bard, A. J. *J. Electroanal. Chem.* 1988, 239, 441. (d) Yamamura, K.; Kominami, K.; Okada, Y.; Ono, S.; Tabushi, I. *Tetrahedron Lett.* 1987, 28, 6475. (e) Diaz, A.; Kaifer, A. E. *J. Electroanal. Chem.* 1988, 249, 333. (f) Tricot, Y. M.; Manassen, J. *J. Phys. Chem.* 1988, 92, 5239. (g) Nishimoto, S.; Kagiya, T.; Kawamura, T.; Lu, Y.; Ye, M. *Radiat. Phys. Chem.* 1988, 32, 727.

(1) (a) Michaelis, L. *Biochem. Z.* 1932, 250, 564. (b) Michaelis, L.; Hill, E. S. *J. Gen. Physiol.* 1933, 16, 859.

(2) Bird, C. L.; Kuhn, A. T. *Chem. Soc. Rev.* 1981, 10, 49.

(3) (a) Mandler, D.; Willner, I. *J. Chem. Soc., Perkin Trans. 2* 1988, 997. (b) Nagamura, T.; Sakai, K. *J. Chem. Soc., Faraday Trans. 1* 1988, 84, 3529. (c) Hamity, M.; Lema, R. H. *Can. J. Chem.* 1988, 66, 1552. (d) Usai, Y.; Sasaki, Y.; Ishii, Y.; Tokumaru, K. *Bull. Chem. Soc. Jpn.* 1988, 61, 3335. (e) Hoffman, M. Z. *J. Phys. Chem.* 1988, 92, 3458. (f) Nosaka, Y.; Miyama, H.; Terauchi, M.; Kobayashi, T. *J. Phys. Chem.* 1988, 92, 255.

(4) Nosaka, Y.; Fox, M. A. *J. Phys. Chem.* 1988, 92, 1893.

(5) (a) Atherton, S. J.; Hubig, S. M.; Callan, T. J.; Duncanson, J. A.; Snowden, P. T.; Rogers, M. A. J. *J. Phys. Chem.* 1987, 91, 3137. (b) Poulos, A. T.; Kelley, C. K.; Simone, R. J. *J. Phys. Chem.* 1981, 85, 823. (c) Barnett, J. R.; Hopkins, A. S.; Ledwith, A. *J. Chem. Soc., Perkin Trans. 2*, 1973, 80. (d) Ebbesen, T. W.; Ferraudi, G. *J. Phys. Chem.* 1983, 87, 3717. (e) Ebbesen, T. W.; Manring, L. E.; Peters, K. S. *J. Am. Chem. Soc.* 1984, 106, 7400.

(6) (a) Anderson, R. F.; Patel, K. B. *J. Chem. Soc., Faraday Trans. 1* 1984, 80, 2693. (b) Howes, K. R.; Pippin, C. G.; Sullivan, J. C.; Meisel, D.; Espenson, J. H. *Inorg. Chem.* 1988, 27, 2932. (c) Patterson, L. K.; Small, R. D.; Scaiano, J. C. *Radiat. Res.* 1977, 72, 218. (d) Farrington, J. A.; Ebert, M.; Land, E. J. *J. Chem. Soc., Faraday Trans. 1* 1978, 74, 665. (e) Rao, P. S.; Hayon, E.; *J. Am. Chem. Soc.* 1974, 96, 1287.

(7) (a) Heyrovsky, M. *J. Chem. Soc., Chem. Commun.* 1987, 1856. (b) Imabayashi, S. I.; Kitamura, N.; Tazuke, S.; Tokuda, K. *J. Electroanal. Chem.* 1988, 243, 143.

(8) (a) Summers, L. A. *The Bipyridinium Herbicides*; Academic: London, 1980. (b) Fedtke, C. *Biochemistry and Physiology of Herbicide Action*; Springer-Verlag: Berlin, 1982.

(9) (a) Kalyanasundaram, K. *Coord. Chem. Rev.* 1982, 46, 159. (b) Whitten, D. G. *Accts. Chem. Res.* 1980, 13, 83. (c) Harriman, A.; West, M. A., Eds. *Photogeneration of Hydrogen*; Academic Press: New York, 1982.

(10) For the applications of methylviologen in solid-state devices, see: (a) Natan, M. J.; Mallouk, T. E.; Wrighton, M. S. *J. Phys. Chem.* 1987, 91, 648. (b) Nagamura, T.; Sakai, K.; Ogawa, T. *J. Chem. Soc., Chem. Commun.* 1988, 1035. (c) Schott, C. J.; Ponjée, J. J.; van Dam, H. T.; van Doorn, R. A.; Bolwijn, P. T. *Appl. Phys. Lett.* 1973, 23, 64. (d) Bruinink, J.; Kregting, C. G. A.; Ponjée, J. J. *J. Electrochem. Soc.* 1977, 124, 1854. (e) Cieslinski, R. C.; Armstrong, N. R. *J. Electrochem. Soc.* 1980, 127, 2605. (f) Wrighton, M. S. *Comments Inorg. Chem.* 1985, 4, 269.

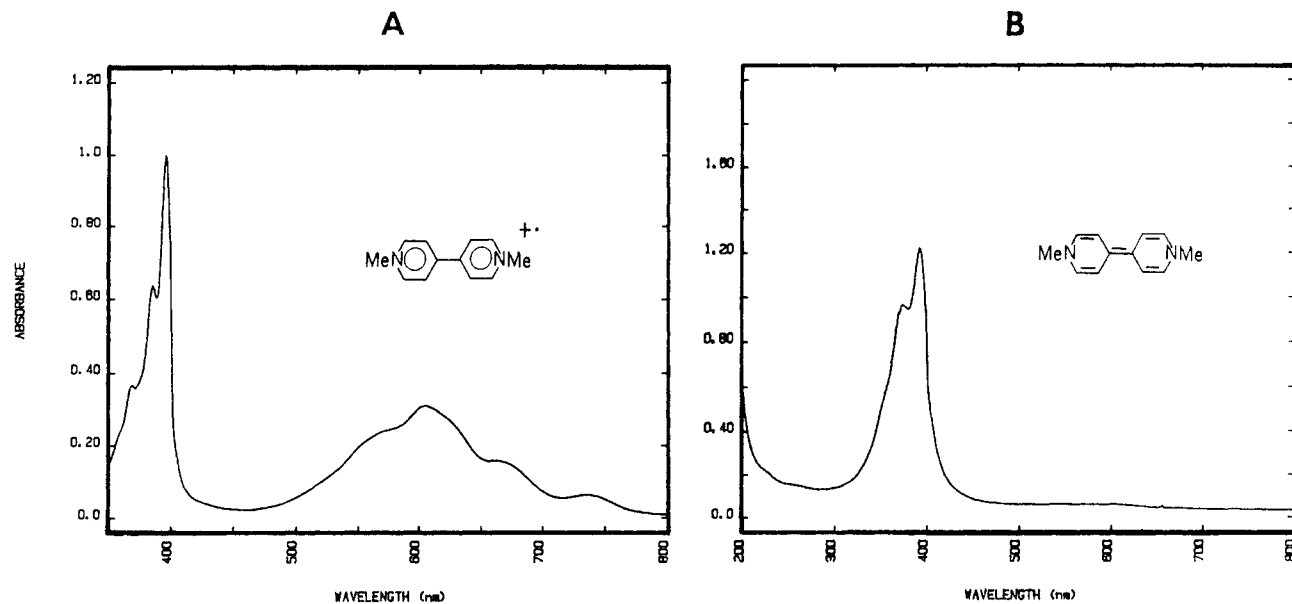


Figure 1. Absorption spectrum of (A) 5×10^{-5} M $MV^{+}PF_6^{-}$ and (B) 3×10^{-4} M MV^0 in dichloromethane.

is singularly absent in both species. Owing to the irreversible precipitation of MV^0 from aqueous solution, the reported value of E^0 for the second redox equilibrium,² i.e., $MV^{2+} + e \rightleftharpoons MV^0$, is questionable.¹⁷ Accordingly, our task was to prepare both of the reduced forms of methylviologen in crystallographically pure form for X-ray diffraction studies and to establish the redox equilibria among MV^{2+} , MV^{+} , and MV^0 . In this report we describe the use of dichloromethane and acetonitrile as the critical aprotic solvents to achieve these ends. Especially relevant is the successful isolation of single crystals of $MV^{+}PF_6^{-}$ that represent the first example of a new class of paramagnetic salts related to organic metals.¹⁸

Results and Discussion

Single-Crystal Synthesis of the Reduced Methylviologens $MV^{+}PF_6^{-}$ and MV^0 . The colorless aqueous solution of 0.1 M methylviologen dichloride ($MVCl_2$) turned dark blue-purple immediately upon the introduction of alkaline dithionite (1 equiv) under an argon atmosphere.¹⁹ The subsequent addition of ammonium hexafluorophosphate to the deeply colored solution resulted in the spontaneous deposition of a dark purple powder accompanied by the bleaching of the supernatant aqueous solution. The highly air-sensitive powder was collected by filtration under an argon atmosphere and carefully crystallized from a mixture of acetonitrile and diethyl ether (see the Experimental Section for details) to yield deep purplish-black needles suitable for single-crystal X-ray crystallography (vide infra). Dissolution of the crystals in thoroughly deaerated dichloromethane resulted in an intensely colored, royal blue solution, the absorption spectrum in Figure 1A showing a pair of prominent bands at λ_{max} 398 and 608 nm with extinction coefficients of $\epsilon = 43\,100$ and $13\,500\text{ M}^{-1}\text{ cm}^{-1}$, respectively. Identical spectra were also obtained in tetrahydrofuran and acetonitrile. The coincidence of the measured extinction coefficient in the latter solvent (Table I) with that determined earlier

Table I. Electronic (UV-Vis) Absorption Spectrum of MV^{+} in Solution^a

solvent	λ_{max}^b , nm	ϵ^b , $\text{M}^{-1}\text{ cm}^{-1}$
MeCN	396 (396)	41 500 (41 800)
	608 (608)	13 500 (13 900)
CH_2Cl_2	398	43 100
	608	13 500
THF	398	42 900
	608	14 100

^a As PF_6^{-} salt in 10^{-4} M solutions at 25 °C. ^b Value in parentheses taken from ref 20.

for MV^{+} from a spectroelectrochemical study²⁰ provided an assay of >99% $MV^{+}PF_6^{-}$ for the dark purple crystals.

The neutral reduced form of methylviologen was synthesized from MV^{+} by the addition of a further equivalent of alkaline dithionite under an argon atmosphere to the deep blue-purple aqueous solution described above.¹² The gradual bleaching of the aqueous solution over the course of several hours was accompanied by the deposition of red crystals, the absorption spectrum of which (Figure 1B) showed the complete disappearance of the prominent low-energy band present in the precursor. Careful recrystallization of the air-sensitive crystals from a mixture of toluene and hexane (see the Experimental Section) yielded dark red prismatic crystals suitable for X-ray crystallography.

Oxidation-Reduction of Methylviologen and Its Reduced Forms. The availability of all three methylviologens MV^0 , MV^{+} , and MV^{2+} in pure form allowed their redox properties to be examined individually by cyclic voltammetry under uniform conditions in acetonitrile containing 0.1 M tetra-*n*-butylammonium perchlorate (TBAP) as the supporting electrolyte. The initial positive-scan cyclic voltammogram of MV^0 at the standard scan rate of $v = 500\text{ mV s}^{-1}$ is shown in Figure 2A, and the values of the anodic and cathodic peak potentials are included as E_p^a and E_p^c , respectively, in Table II. For comparison, Figures 2B and 2C show the initial negative-scan cyclic voltammograms of MV^{+} and MV^{2+} under the same conditions. The ratios of the anodic and cathodic peak currents of unity and the separations of the peak potentials $\Delta E_p \sim 60\text{ mV}$ in all three cyclic voltammograms

(16) (a) Creasy, K. E.; Shaw, B. R. *Electrochim. Acta* 1988, 33, 551. (b) Li, Z. Y.; Mallouk, T. E.; Persaud, L.; Wang, C. M. *J. Phys. Chem.* 1988 92, 2592. See also ref 11.

(17) Owing to problems associated with adsorption on the cathode.

(18) Torrance, J. B. *Acc. Chem. Res.* 1979, 12, 79.

(19) For kinetics of reduction, see: Tsukahara, K.; Wilkins, R. G. *J. Am. Chem. Soc.* 1985, 107, 2632.

(20) Watanabe, T.; Honda, K. *J. Phys. Chem.* 1982, 86, 2617.

Table II. Redox Potentials of Methylviologen and of Its Reduced Forms^a

starting material	solvent	first couple			second couple			ref
		$-E_p^c$	$-E_p^a$	$-E_{1/2}$	$-E_p^c$	$-E_p^a$	$-E_{1/2}$	
MV ⁰	MeCN	0.430	0.368	0.399	0.844	0.778	0.811	b
MV ^{•+} PF ₆ ⁻	MeCN	0.433	0.374	0.404	0.855	0.791	0.823	b
MV ²⁺ (PF ₆ ⁻) ₂	CH ₂ Cl ₂	0.353 ^c	0.248	-	0.806	0.701	0.753	b
	MeCN	0.441	0.378	0.409	0.858	0.790	0.824	b
	MeCN ^d			0.440			0.864	e
	DMF ^d			0.424			0.844	e
Cp ₂ Fe	H ₂ O			0.687			1.112	f
	MeCN	-0.385	-0.468	-0.426				b

^aBy cyclic voltammetry of 5×10^{-3} M solutions containing 0.1 M TBAP at $v = 0.5$ V s⁻¹ at 25 °C, unless indicated otherwise. All potentials references to aqueous SCE. ^bThis work. ^cAdsorption wave. ^dBy polarography. ^eReference 25. ^fReference 2.

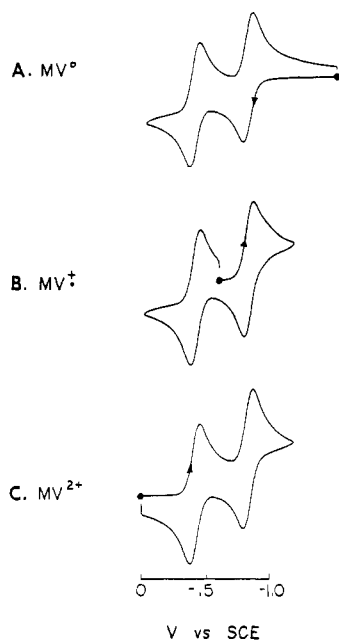
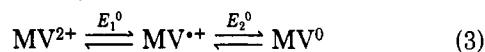


Figure 2. Cyclic voltammograms of (A) MV⁰ on the initial positive scan, (B) MV^{•+}PF₆⁻, and (C) MV²⁺(PF₆⁻)₂ on the initial negative scan in acetonitrile containing 0.1 M TBAP.

indicate that the redox equilibria among the three species are electrochemically reversible,²¹ i.e.



Furthermore, the thermodynamic potential for the equilibria in eq 3 (given as $(E_1^0 + E_2^0)/2$)²² is constant at $E_1^0 = -0.430 \pm 0.005$ and $E_2^0 = -0.835 \pm 0.008$ V vs SCE in acetonitrile, by calibration relative to the ferrocene standard.²³ For completeness, Table II also includes the values of the redox potentials starting from MV²⁺ in various solvents, as taken from the pertinent literature.^{2,25} For the electrochemical measurements in various solvents, cognizance must always be taken for the possibility of electrode adsorption in various solvents, e.g., MV²⁺ in dichloromethane²⁶ (entry 3) and MV⁰ in water¹⁷ (entry 7).

(21) Bard, A. J.; Faulkner, L. R. *Electrochemical Methods*; Wiley: New York, 1980.

(22) Howell, J. O.; Goncalves, J. M.; Amatore, C.; Klasinc, L.; Wightman, R. M.; Kochi, J. K. *J. Am. Chem. Soc.* 1984, 106, 3968.

(23) After correction of the value for ferrocene in Table II to +0.40 V vs SCE as suggested in ref 24.

(24) Gagne, R. R.; Koval, C. A.; Lisensky, G. C. *Inorg. Chem.* 1980, 19, 2854. See also: Gritzner, G.; Kuta, J. *Pure Appl. Chem.* 1983, 56, 461. Note that the Cp₂Fe/Cp₂Fe⁺ couple is not Nernstian (Connelly, N. G.; Geiger, W. E. *Adv. Organomet. Chem.* 1984, 23, 1).

(25) Compare Hunig, S.; Gross, J. *Tetrahedron Lett.* 1968, 21, 2599 for a polarographic study in CH₃CN.

(26) The initial positive-scan cyclic voltammogram of MV^{•+}PF₆⁻ in dichloromethane shows on the return cathodic wave for MV²⁺ as an adsorption peak (see ref 21, p 525ff).

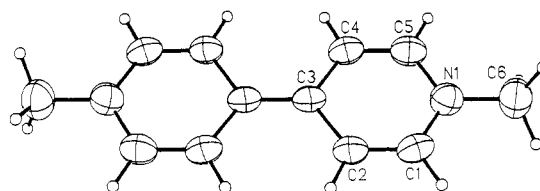


Figure 3. ORTEP diagram of MV⁰ including the numbering scheme in one ring (The other ring atoms designated by primes in Table III and VIII).

Table III. Selected Bond Distances (Å) and Bond Angles (deg) for MV⁰

Bond Lengths, Å			
N(1)-C(1)	1.375 (7)	N(1)-C(5)	1.387 (6)
N(1)-C(6)	1.447 (8)	N(2)-C(7)	1.382 (6)
N(2)-C(11)	1.383 (7)	N(2)-C(12)	1.451 (5)
C(1)-C(2)	1.325 (8)	C(2)-C(3)	1.461 (6)
C(3)-C(4)	1.444 (7)	C(3)-C(3')	1.363 (9)
C(4)-C(5)	1.336 (8)	C(7)-C(8)	1.329 (7)
C(8)-C(9)	1.465 (6)	C(9)-C(10)	1.452 (5)
C(9)-C(9')	1.370 (7)	C(10)-C(11)	1.330 (7)
Bond Angles, deg			
C(1)-N(1)-C(5)	116.4 (4)	C(1)-N(1)-C(6)	122.7 (4)
C(5)-N(1)-C(6)	120.9 (4)	C(7)-N(2)-C(11)	116.5 (4)
C(7)-N(2)-C(12)	121.2 (4)	C(11)-N(2)-C(12)	121.8 (4)
N(1)-C(1)-C(2)	123.8 (4)	C(1)-C(2)-C(3)	122.6 (4)
C(2)-C(3)-C(4)	111.2 (4)	C(2)-C(3)-C(3')	123.9 (5)
C(4)-C(3)-C(3')	124.9 (5)	C(3)-C(4)-C(5)	124.0 (4)
N(1)-C(5)-C(4)	121.9 (5)	N(2)-C(7)-C(8)	122.5 (4)
C(7)-C(8)-C(9)	123.3 (4)	C(8)-C(9)-C(10)	111.5 (3)
C(8)-C(9)-C(9')	123.7 (5)	C(10)-C(9)-C(9')	124.8 (5)
C(9)-C(10)-C(11)	122.7 (4)	N(2)-C(11)-C(10)	123.5 (4)

X-ray Crystallography of the Reduced Methylviologens MV⁰ and MV^{•+}PF₆⁻. The red crystal of MV⁰ in the monoclinic space group $P2_1/c$ with $a = 14.449$ (5) Å, $b = 5.953$ (2) Å, and $c = 13.542$ (5) Å and $\beta = 115.96$ (3)° consisted of pairs of nearly identical planar molecules situated about inversion centers in the unit cell. The interplanar separation of ~6 Å between MV⁰ molecules precludes any conformational distortion arising from lattice effects. Figure 3 shows the ORTEP diagram of MV⁰ from the top perspective to emphasize the essential retention of the methylviologen skeletal framework. However the bond distances listed in Table III indicate a marked alternation of carbon-carbon bond lengths around each heterocyclic moiety so that C1-C2 (1.33 Å), C4-C5 (1.34 Å), and C3-C3' (1.36 Å) can all be simply considered as localized double bonds and C2-C3 (1.46 Å) and C3-C4 (1.44 Å) as localized single bonds. Such alternating bond lengths are the same as those found in the analogous planar structures of the dipyrans and dithiopyrans shown below,^{27,28}

(27) Chasseau, D.; Gaultier, J.; Hauw, C.; Fugnitto, R.; Gianis, V.; Strzelecka, H. *Acta Crystallogr.* 1982, B38, 1629.

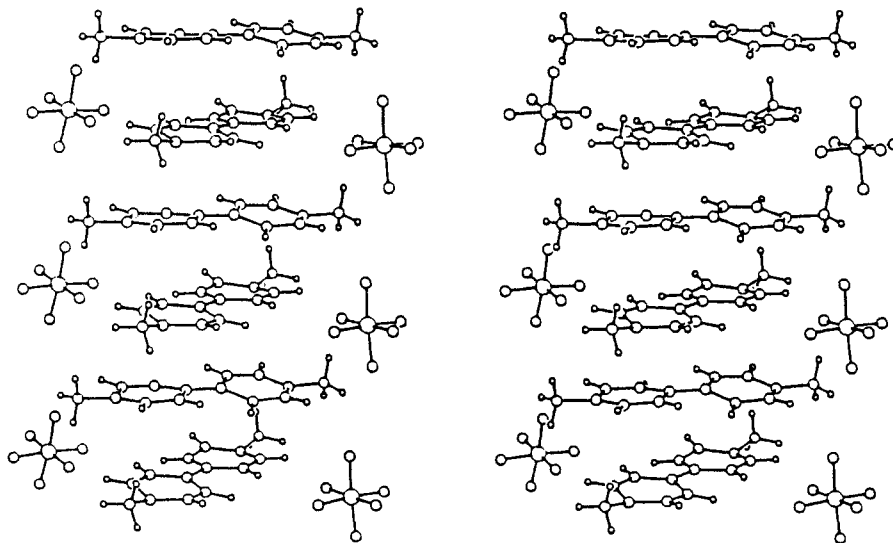
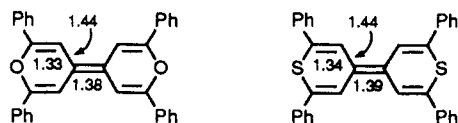


Figure 4. Stereoscopic view of the cation/anion stacking along the *c* axis of the unit cell of $MV^{2+}PF_6^{-}$.

Table IV. Selected Bond Distances (Å) and Bond Angles (deg) for $MV^{2+}PF_6^{-}$

Bond Angles, deg			
F(2)–P–F(1)	89.9 (4)	F(3)–P–F(1)	177.8 (7)
F(3)–P–F(2)	92.0 (5)	F(4)–P–F(1)	89.8 (5)
F(4)–P–F(2)	175.7 (8)	F(4)–P–F(3)	88.5 (6)
F(5)–P–F(1)	84.0 (9)	F(5)–P–F(5)	90.8 (7)
F(5)–P–F(3)	94.7 (8)	F(5)–P–F(4)	93.5 (8)
F(6)–P–F(1)	98.7 (8)	F(6)–P–F(2)	85.9 (7)
F(6)–P–F(3)	82.7 (9)	F(6)–P–F(4)	89.9 (7)
F(6)–P–F(5)	175.7 (6)	C(5)–N(1)–C(1)	118.2 (9)
C(6)–N(1)–C(1)	121.3 (10)	C(6)–N(1)–C(5)	119.7 (9)
C(2)–C(1)–N(1)	123.3 (9)	C(3)–C(2)–C(1)	119.4 (9)
C(4)–C(3)–C(2)	114.6 (8)	C(2)–C(3)–C(3')	122.8 (9)
C(4)–C(3)–C(3')	122.4 (9)	C(5)–C(4)–C(3)	121.8 (10)
C(4)–C(5)–N(1)	121.8 (10)	C(11)–N(2)–C(7)	117.3 (8)
C(12)–N(2)–C(7)	119.7 (8)	C(12)–N(2)–C(11)	118.6 (8)
C(8)–C(7)–N(2)	119.5 (9)	C(9)–C(8)–C(7)	122.3 (9)
C(10)–C(9)–C(8)	114.7 (8)	C(8)–C(9)–C(9')	120.9 (9)
C(10)–C(9)–C(9')	124.3 (9)	C(11)–C(10)–C(9)	123.1 (9)
C(10)–C(11)–N(2)	120.7 (9)		
Bond Lengths, Å			
P–F(1)	1.478 (7)	P–F(2)	1.552 (6)
P–F(3)	1.470 (8)	P–F(4)	1.530 (7)
P–F(5)	1.545 (9)	P–F(6)	1.499 (10)
N(1)–C(1)	1.343 (11)	N(1)–C(5)	1.370 (12)
N(1)–C(6)	1.494 (12)	C(1)–C(2)	1.353 (13)
C(2)–C(3)	1.439 (12)	C(3)–C(4)	1.437 (12)
C(3)–C(3')	1.399 (12)	C(4)–C(5)	1.329 (12)
N(2)–C(7)	1.385 (11)	N(2)–C(11)	1.388 (11)
N(2)–C(12)	1.495 (11)	C(7)–C(8)	1.356 (12)
C(8)–C(9)	1.401 (11)	C(9)–C(10)	1.396 (12)
C(9)–C(9')	1.444 (12)	C(10)–C(11)	1.331 (11)

and they reveal the nonaromatic, polyene-like structure of MV^0 .



The almost black crystal of $MV^{2+}PF_6^{-}$ in the orthorhombic space group $Pnn2$ with $a = 12.773$ (3) Å, $b = 16.902$ (5) Å, and $c = 6.578$ (2) Å consisted of separate cation/anion stacks of MV^{2+} and PF_6^{-} , as shown in the stereoscopic view of the unit cell in Figure 4. A closer

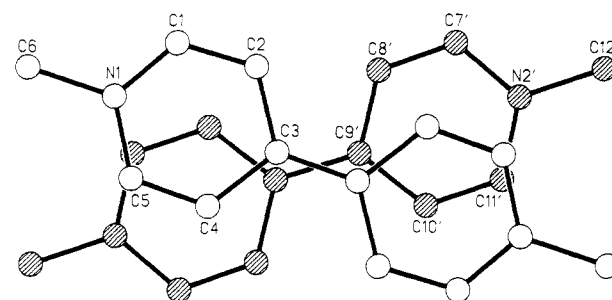
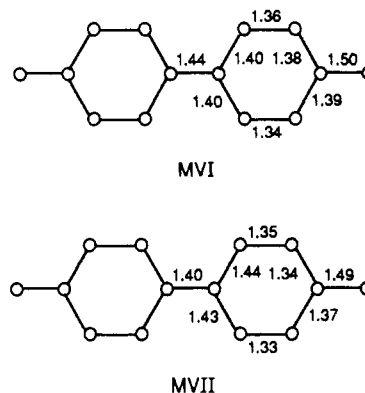


Figure 5. Top perspective showing the relative orientation of MVI and MVII moieties in crystalline $MV^{2+}PF_6^{-}$. Hydrogen atoms are omitted for clarity.

inspection of the MV^{2+} stack revealed two distinct types of cationic structures that are hereafter designated MVI and MVII. The most noteworthy difference between these



moieties is the central bond distance of 1.44 Å in MVI (Table IV), which is considerably longer than 1.40 Å in MVII—reminiscent of the similar difference between MV^{2+} (1.48 Å) and MV^0 (1.36 Å). Moreover MVI and MVII deviate significantly from the coplanar structures of MV^{2+} and MV^0 , as described in detail in the Experimental Section. The cations are oriented in the infinite stack at an angle of 37° relative to one another (Figure 5); but a single distance of 3.29 Å that uniformly separates MVI and MVII indicates no tendency for their selective pairwise interaction in the crystal.

Spectroscopic Properties of $MV^{2+}PF_6^{-}$ in the Crystalline State. In order to probe the unique segregation of cation radical structures as MVI and MVII in

(28) Luss, H. R.; Smith, D. L. *Acta Crystallogr.* 1980, B36, 1580. See also Isett, L. C.; Reynolds, G. A.; Schneider, D.; Perlstein, J. H. *Solid State Commun.* 1979, 30, 1.

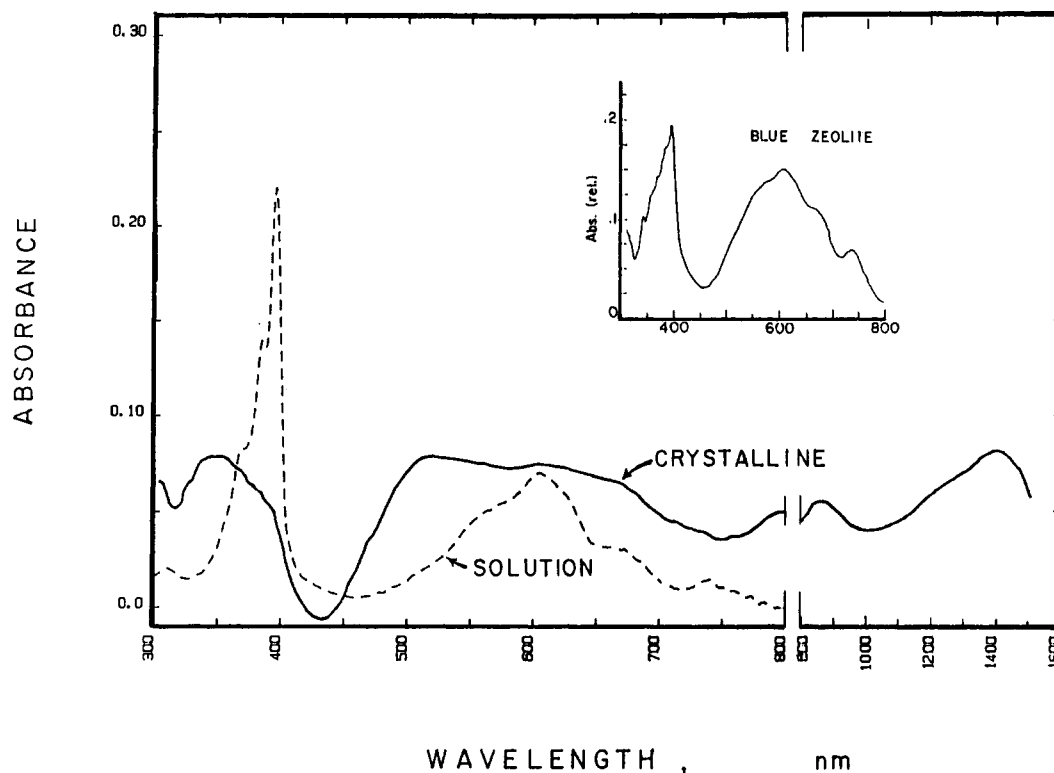


Figure 6. Diffuse reflectance spectrum of crystalline $MV^{++}PF_6^-$ in an alumina matrix (—), in comparison with that of monomeric MV^{++} in (blue) zeolite in the inset and in acetonitrile solution (---).

crystalline $MV^{++}PF_6^-$, the spectroscopic properties of the bulk material were compared with those of the isolated cation MV^{++} , both in a solid matrix and in solution. For example, Figure 6 presents the diffuse reflectance spectrum of crystalline $MV^{++}PF_6^-$ (as a 1% dispersion in alumina) showing three principal bands, a resolved band with $\lambda_{max} = 350$ nm and a pair of unresolved low-energy bands with $\lambda_{max} \sim 520$ and 650 nm. This differs substantially from the diffuse reflectance spectrum of MV^{++} isolated in a zeolite matrix (see inset).¹¹ It is noteworthy that the latter is essentially the same as the absorption spectrum of MV^{++} dissolved in dichloromethane solution (Figure 1A). Such a marked spectral difference is clearly associated with interionic effects in crystalline $MV^{++}PF_6^-$ that are absent in the separated cation radicals. Further spectroscopic indications of interionic effects show up in the vibrational spectrum of MV^{++} in the crystalline material that is different from that in solution²⁹ and in $CdPS_3$ matrix.³⁰ For example, the diagnostic C=C stretching bands³¹ at 1600, 1533, 1357, 1211, 1029, and 817 cm^{-1} for MV^{++} in 10^{-4} M aqueous solution and at the unshifted frequencies of 1597, 1528, 1349, 1218, 1029 and 809 cm^{-1} for MV^{++} in the $CdPS_3$ matrix appeared at 1644, 1606, 1341, 1201, 1030, and 815 cm^{-1} in crystalline $MV^{++}PF_6^-$. Importantly, the latter are the same as those previously found for cation radical salts of methylviologen that were electrochemically deposited as thin films.^{29,32}

The relevance of cation radical structures in crystalline $MV^{++}PF_6^-$ is shown by the EPR spectrum in Figure 7. The anisotropy of the EPR spectrum with $g_{\parallel} = 2.0010$ and $g_{\perp} = 2.0036$ for axial symmetry³³ contrasted with the

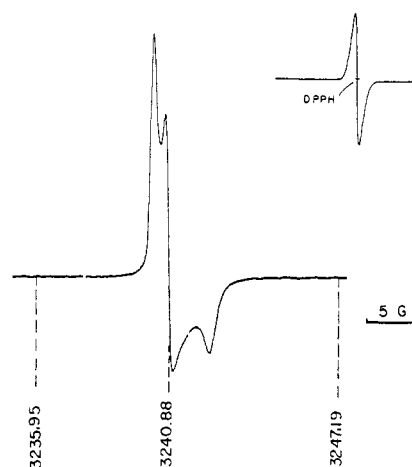


Figure 7. EPR spectrum of polycrystalline $MV^{++}PF_6^-$ with 1H NMR field markers in gauss. The inset shows the isotropic spectrum of monomeric MV^{++} in the blue zeolite (see Figure 6).

isotropic spectrum obtained for MV^{++} isolated in a zeolite matrix¹¹ (see inset). Moreover the g value of (g) = 2.0027 is the same as that previously found in the well-resolved EPR spectrum of MV^{++} in aqueous solution with $\langle g \rangle = 2.003$.³⁴ However, the magnitude of the electronic coupling among the cation radical moieties in the crystalline lattice is sufficient to lead to bulk diamagnetism i.e. $\mu_{eff} \sim 0$ (see the Experimental Section).

Discussion

The redox properties of methylviologen as the quintessential electron mediator in aqueous solution is amplified in this study by the establishment of the reversible equilibria (eq 3) in nonaqueous solution, the extensive use of which has allowed both of the relevant reduced forms

(29) Lu, T.; Cotton, T. M.; Hurst, J. K.; Thompson, D. H. P. *J. Phys. Chem.* 1988, 92, 6978.

(30) Poizat, O.; Sourisseau, C.; Corset, J. *J. Mol. Struct.* 1986, 143, 203.

(31) Ghoshal, S.; Lu, T.; Feng, Q.; Cotton, T. M. *Spectrochimica Acta* 1988, 44A, 651.

(32) Ito, M.; Sasaki, H.; Takahashi, M. *J. Phys. Chem.* 1987, 91, 3932.

(33) Symons, M. C. R. *Chemical and Biochemical Aspects of Electron-Spin Resonance Spectroscopy*; Wiley: New York, 1978; p 28ff.

(34) Rieger, A. L.; Rieger, P. H. *J. Phys. Chem.* 1984, 88, 5845.

Table V. Vibrational Spectral Data of Methylviologen Cation Radical in the Solid State and in Dilute Solution

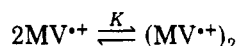
MV ^{•+} PF ₆ ^{-a}	(MV ^{•+}) ₂ ^b	MV ^{•+c}
1644	1641 (1643)	1600 (1597)
1606	1605	1533 (1528)
1514	1511	
1341	1340 (d)	1357 (1349)
1201	1200 (d)	1211 (1218)
—	1185 (1185)	1201 (1194)
1030	— (1050)	1029 (1029)
815		817 (809)

^aIn wavenumbers; MV^{•+}PF₆⁻ in KBr. ^bAdsorbate on electrode from ref 32 (ref 29). ^cIn dilute aqueous from ref 29 or in solid CdPS₃ matrix from ref 30 in parentheses. ^dTwin bands at 1297 and 1240 cm⁻¹.

MV⁰ and MV^{•+} to be isolated and their molecular structures crystallographically characterized for the first time.

The most reduced form of methylviologen MV⁰ is a potent electron donor by virtue of its value for $E^0 = -0.84$ V. As such, it compares favorably with other powerful enamines such as tetrakis(dimethylamino)ethylene³⁵ and 1,4-bis(trialkylsilyl)-1,4-dihydropyrazines³⁶ in electron-transfer processes. Furthermore, MV⁰ readily forms a series of charge-transfer salts with various electron acceptors such as tetracyanoquinodimethane (TCNQ), chloranil, bis(benzene)iron(II) dication, etc., that have potential as organic metals.³⁷ In the crystalline state MV⁰ exists as separate planar molecules similar to that found in crystalline anthracene.³⁸ Thus there is no spectral feature of MV⁰ in the crystalline state that differs in any significant way from that found in solution.

In marked contrast to MV⁰, the purple-black crystals of methylviologen cation radical MV^{•+}PF₆⁻ are visually distinct from the royal blue color of saline nonaqueous solutions. The different colors arise in the electronic spectra by the appearance of a new band with $\lambda_{\max} \sim 530$ nm (Figure 6) that is absent in the spectrum of monomeric MV^{•+}, either dissolved in dichloromethane solution (Figure 1A) or incorporated into a zeolite matrix (Figure 6 inset). The latter indicates that the new band is not a solid-state effect, but results specifically from aggregation. Indeed the new band is strikingly akin to that with $\lambda_{\max} = 537$ nm previously assigned to the dimer cation radical (MV^{•+})₂ by the digital deconvolution of a series of spectra obtained in concentrated aqueous solutions.³⁹ It is important to note that the spectrophotometric determination of the formation constant of the dimer cation radical, i.e.



of $K = 6 \times 10^2 \text{ M}^{-1}$ in water must be substantially larger

than that in nonaqueous media. Thus the highly colored solutions of MV^{•+} in dichloromethane and acetonitrile remain royal blue (compare Figure 1A) without the purple coloration characteristic of concentrated aqueous solutions,⁴⁰ even up to the concentration limits at which the salts begin to precipitate. Additional evidence for the similarity of crystalline MV^{•+}PF₆⁻ with solution-state dimers (MV^{•+})₂ is obtained by the comparison of their infrared spectra. Table V lists the pertinent vibrational bands of crystalline MV^{•+}PF₆⁻ in a KBr matrix together with those previously reported for dimeric MV^{•+} adsorbed on surfaces.^{29,30,32} The striking coincidences of all the stretching (columns 1–3) bands are in marked contrast to those found of monomeric MV^{•+} in a solid matrix (column 4) or in dilute aqueous solution (column 5). Since these vibrational spectra establish the structural similarity of crystalline MV^{•+}PF₆⁻ to MV^{•+} dimers (or higher aggregates), the X-ray crystallographic analysis that reveals the presence of infinite MV^{•+} stacks (see Figure 4) must relate to highly interacting forms of MV^{•+} extant in the crystalline material. The latter is underscored by the short interionic separation of ~ 3.3 Å that uniformly separates alternate layers of the nonidentical cations MVI and MVII throughout the crystal.

Considerable structural information is available for various salts of the parent methylviologen MV²⁺ in combination with structurally distinct counterions. Table VI presents a partial collation of the pertinent structural parameters for MV²⁺ present in diverse salts.^{41–47} Clearly the minor excursions of the bond lengths from the average values are insufficient to account for the significant difference between those in MVI and MVII, included as entries 11 and 12 for comparison.

A closer examination of the structural data reveals that the bond lengths in MVI and MVII are intermediate between those found in MV²⁺ and MV⁰ (entry 13). Indeed the mean length of each bond in MV^{•+} (i.e., the average of that in MVI and MVII) is almost identical with the arithmetic average of the corresponding bond length in MV⁰ and MV²⁺, each bond in MVI being displaced from its mean value toward MV²⁺ and that in MVII being displaced toward MV⁰. Particular emphasis should be directed to the interannular separations—the central carbon-carbon bond of 1.48 Å in MV²⁺ is equivalent to a single bond between sp² centers and 1.36 Å in MV⁰ is equivalent to a double bond, both in comparison with the significant difference of 1.44 and 1.40 Å in MVI and MVII, respectively.

The structural differentiation between MVI and MVII forms in crystalline MV^{•+}PF₆⁻ are best accommodated by a partial disproportionation toward MV⁰ and MV²⁺. We

Table VI. Structural Parameters of Methylviologen and Its Reduced Forms

	bond distance, Å					ref
	C1-C2	C2-C3	C3-C3'	N-CH ₃	N-C1	
MV ²⁺ (Cl ⁻) ₂	1.38	1.37	1.47	1.41	1.34	41
MV ²⁺ (Br ⁻) ₂	1.37	1.39	1.45	1.47	1.34	41
MV ²⁺ (I ⁻) ₂	1.38	1.39	1.48	1.45	1.34	41
MV ²⁺ CuCl ₄ ²⁻	1.37	1.39	1.47	1.47	1.34	42
MV ²⁺ Cu ₂ Cl ₆ ²⁻	1.38	1.39	1.49	1.48	1.35	43
MV ²⁺ Ni[S ₂ C ₂ (CN) ₂] ₂ ²⁻	1.37	1.38	1.49	1.49	1.34	44
MV ²⁺ C ₄ (CN) ₆ ²⁻	1.35	1.39	1.48	1.48	1.34	45
MV ²⁺ (TCNQ) ₃ ²⁻	1.37	1.39	1.48	1.49	1.34	46
MV ²⁺ Ni(CN) ₄ ²⁻	1.40	1.40	1.47	1.51	1.34	47
MV ^{•+} PF ₆ ⁻						
MVI	1.34	1.40	1.44	1.50	1.39	a
MVII	1.34	1.44	1.40	1.49	1.36	a
MV ²⁺ (DMN)(PF ₆ ⁻) ₂ ^b	1.36	1.39	1.48	1.48	1.34	48
MV ⁰	1.32	1.46	1.36	1.45	1.38	a

^aThis work. ^bCharge-transfer complex of MV²⁺(PF₆⁻)₂ with 2,6-dimethoxynaphthalene.

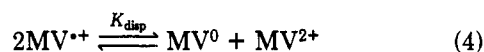
Table VII. Calculated Disproportionation Constants for Methylviologen Cation Radical in Solution^a

solvent	K_{disp}	ΔG_{disp} , kcal mol ⁻¹
H ₂ O ^b	4.5×10^{-8}	10.0
DMF ^c	7.7×10^{-8}	9.7
CH ₃ CN	11×10^{-8}	9.5
CH ₂ Cl ₂ ^d	2.5×10^{-8}	10.4

^aBased on the redox potentials in Table II. ^bReference 2. ^cReference 25. ^dApproximation owing to electrode absorption (see ref 26).

judge (solely from the differences in bond lengths) that roughly one-quarter of an electron is transferred to yield the oxidized MVI and the reduced MVII as alternating forms in the MV^{•+} stack (Figure 4). The accompanying deviations of MVI and MVII from planarity can be attributed to Jahn-Teller distortions in the cation radical salt.^{49,50} Be that as it may, the intracrystalline disproportionation observed in MV^{•+}PF₆⁻ is unique. Unfortunately, the paucity of structural information for other organic cation radical salts (in contrast to numerous reports of a variety of mixed valence salts⁵¹) limits the extensive comparison of this unusual phenomenon. It should be noted however that the cation radical salts of the widely studied donor tetrathiafulvalene (TTF) show no signs of disproportionation in their isolated dimeric (TTF^{•+})₂ units.⁵²

The equilibrium constant for disproportionation of MV^{•+} in solution, i.e.



(35) (a) Kuwata, K.; Geske, D. H. *J. Am. Chem. Soc.* **1964**, *86*, 2101. (b) Cetinkaya, B.; King, G. H.; Krishnamurty, S. S.; Lappert, M. F.; Pedley, J. B. *J. Chem. Soc., Chem. Commun.* **1971**, 1370.

(36) (a) Kaim, W. *Angew. Chem., Int. Ed. Engl.* **1984**, *23*, 613. (b) Baumgarten, J.; Bessenbacher, C.; Kaim, W.; Stahl, T. *J. Am. Chem. Soc.* **1989**, *111*, 2126.

(37) Bockman, T. M., unpublished results.

(38) Silinsh, E. A. *Organic Molecular Crystals*; Springer-Verlag: New York, **1980**; p 10ff.

(39) Stargardt, J. F.; Hawkrige, F. M. *Anal. Chim. Acta* **1983**, *146*, 1.

(40) Thorneley, R. N. F. *Biochem. Biophys. Acta* **1974**, *333*, 487.

(41) Russell, J. H.; Wallwork, S. C. *Acta Crystallogr.* **1972**, *B28*, 1527.

(42) Russell, J. H.; Wallwork, S. C. *Acta Crystallogr.* **1969**, *B25*, 1691.

(43) Murray-Rust, P. *Acta Crystallogr.* **1975**, *B31*, 1771.

(44) Kisch, H.; Fernández, A.; Wakatsuki, Y.; Yamazaki, H. *Z. Naturforsch.* **1985**, *40b*, 292.

(45) Nakamura, K.; Kai, Y.; Yasuoka, N.; Kasai, N. *Bull. Chem. Soc. Jpn.* **1981**, *54*, 3300.

(46) Ashwell, G. J.; Wallwork, S. C. *Acta Crystallogr.* **1979**, *B35*, 1648.

(47) Basson, S. S.; Bok, L. D. C.; Leipoldt, J. G. *Acta Crystallogr.* **1969**, *B25*, 579.

(48) Yoon, K. B.; Kochi, J. K. *J. Am. Chem. Soc.* **1989**, *111*, 1128.

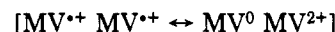
(49) For example, see the Jahn-Teller distortion in benzene cation radical in: (a) Nakajima, T.; Toyota, A.; Kataoka, M. *J. Am. Chem. Soc.* **1982**, *104*, 5610 and references therein. (b) Iwasaki, M.; Toriyama, K.; Numone, K. *J. Chem. Soc., Chem. Commun.* **1983**, 320. See also Shida, T. *Electronic Absorption Spectra of Radical Ions*; Elsevier: New York, **1988**.

(50) Note that the cation/anion separation associated with MVI is significantly less [$r(\text{N}\cdots\text{P}) = 4.80 \text{ \AA}$] than that [$r(\text{N}\cdots\text{P}) = 4.93 \text{ \AA}$] with MVII, in accord with the higher formal charge. In addition, the slight anion-dependent alterations in the bond distances of the MV²⁺ cation in Table VI may be a consequence of structurally diverse (charge-transfer) ion pairing in the crystal reminiscent of that described by Bockman, T. M.; Kochi, J. K. *J. Am. Chem. Soc.* **1985**, *111*, 4669.

(51) Enkelmann, V. In *Polynuclear Aromatic Hydrocarbons Advances in Chemistry* 217; Ebert, L. B.; Ed.; American Chemical Society: Washington, DC, **1988**; p 177ff.

(52) The cation radical of TTF (as the halide salt) exhibits discrete pairing. Scott, B. A.; Laplaca, S. J.; Torrance, J. B.; Silverman, B. D.; Welber, B. *J. Am. Chem. Soc.* **1977**, *99*, 6631.

is predictable from the reversible redox potentials evaluated by cyclic voltammetry (see Table II). The solvent dependence of the highly endergonic driving force ($-\Delta G_{\text{disp}}$) for disproportionation is included in Table VII, together with the computed value of the disproportionation constant.⁵³ The limited value of $K_{\text{disp}} \sim 10^{-7}$ that is consistently evaluated, irrespective of solvent polarity, indicates that the disproportionation of MV^{•+} in the crystalline material is not likely to be driven by any environmental difference that favors MV⁰ and/or MV²⁺. Instead we suggest that the same interionic forces that lead to dimeric (MV^{•+})₂ in aqueous solution are operative in the crystal, namely, charge transfer or self-complexation that is qualitatively describable in terms of valence-bond exchange such as⁵⁴



Such an association is related to the dimerization of neutral pyridinyl radicals for which Kosower and Itoh⁵⁵ found the spectroscopic and magnetic properties to differ from those of the monomeric free radicals in a manner descriptive of charge-transfer complexation. If so, the absence of repulsive electrostatic forces would predict large changes in K_{disp} with variation in solvent polarity.⁵⁶ In a related context, it should be noted that the charge-transfer band observed at $\lambda_{\text{max}} \sim 1400 \text{ nm}$ in the diffuse reflectance spectrum of crystalline MV^{•+}PF₆⁻ (Figure 6), is comparable to that at 1200 nm in K⁺TCNQ⁻.⁵⁷ Interestingly, such a charge-transfer absorption is analogous to the excitation to the conduction band of organic metals,¹⁸ and the energy difference of 0.4 eV is in the range expected for highly conducting organic radical salts.⁵⁸ It has been suggested that (MV^{•+})₂ in solution may have a quinydrone-like structure, as judged by the diminution of the EPR intensity in aqueous solution.³⁴

The strong component of charge-transfer exchange in crystalline MV^{•+}PF₆⁻ differs from that present in weak charge-transfer complexes of methylviologen with aromatic donors,⁵ i.e.



Thus the X-ray crystallographic analysis of the charge-transfer complex of MV²⁺ with 2,6-dimethoxynaphthalene shows no structural alteration in either the methylviologen or aromatic moiety,⁴⁸ in accord with the highly endergonic driving force of >1.5 eV predicted for disproportionation from the strongly positive values of arene redox potentials.²²

Experimental Section

Materials. Methylviologen dichloride (Ortho Chemicals) was recovered from a concentrated aqueous solution and repeatedly recrystallized from methanol until colorless [¹H NMR (D₂O):³⁴ δ 8.89, 8.36 ($J_{\text{AB}} = 8 \text{ Hz}$, 8 H), 4.44 (s, 6 H)]. MVCl₂ was converted

(53) The rate of conproportionation (reverse of eq 4) is very fast ($k \geq 3 \times 10^9 \text{ M}^{-1} \text{ s}^{-1}$) consistent with the large value for $-\Delta G_{\text{disp}}$. See Winograd, N.; Kuwana, T. *J. Am. Chem. Soc.* **1970**, *92*, 224.

(54) Kosower, E. M.; Cotter, J. L. *J. Am. Chem. Soc.* **1964**, *86*, 5521.

(55) (a) Itoh, M.; Nagakura, S. *J. Am. Chem. Soc.* **1967**, *89*, 3959. (b) Itoh, M.; Kosower, E. M. *J. Am. Chem. Soc.* **1967**, *89*, 3655. (c) Itoh, M.; Kosower, E. M. *J. Am. Chem. Soc.* **1968**, *90*, 1843.

(56) The presence of (MV^{•+})₂ in water but not dichloromethane (or acetonitrile) may be attributed to the neutralization of repulsive forces. See also de Sorgo, M.; Wasserman, B.; Szwarc, M. *J. Phys. Chem.* **1972**, *76*, 3468.

(57) Tkacz, M.; Jurgensen, C. W.; Drickamer, H. G. *J. Chem. Phys.* **1986**, *84*, 649.

(58) Wudl, F. *Acc. Chem. Res.* **1984**, *17*, 227. The solid-state properties of MV^{•+} salt are under investigation.

to the hexafluorophosphate salt by dissolution in water followed by the addition of HPF_6 . The colorless precipitate was recrystallized from a mixture of acetonitrile and diethyl ether.⁵⁹ Sodium dithionite (Matheson, Coleman & Bell) and aqueous hexafluorophosphoric acid (Aldrich) were used as received. Dichloromethane (Baker, analytical grade) was distilled from P_2O_5 and redistilled from calcium hydride. Acetonitrile was treated with 0.1% KMnO_4 overnight and refluxed for 1 h, and the MnO_2 removed by filtration. It was distilled from P_2O_5 and redistilled from CaH_2 . Toluene (Baker), hexane (Fisher), diethyl ether, and tetrahydrofuran (Mallinkrodt) were redistilled under an argon atmosphere from sodium, calcium hydride, and lithium aluminum hydride, respectively, prior to use. All organic solvents were stored under an atmosphere of argon. Deionized water was distilled and then degassed by stirring under dynamic vacuum for 30 min.

Methylviologen Hexafluorophosphate ($\text{MV}^{2+}\text{PF}_6^-$). A solution of methylviologen dichloride (MVCl_2 , 1.0 g, 3.9 mmol) in 50 mL of deaerated water was stirred under an argon atmosphere while sodium dithionite (1.35 g, 7.8 mmol) and aqueous 10% ammonia (30 mL) were successively added. The solution became deep violet upon addition of the ammonia solution. The dark solution was stirred for 5 min, and a solution of $\text{NH}_4^+\text{PF}_6^-$ [prepared in situ by the neutralization of 2.0 mL of 60% aqueous HPF_6 followed by dilution to 30 mL] was added. A deep purple precipitate formed immediately, and the supernatant solution turned almost colorless. The air-sensitive purple powder was filtered under an argon atmosphere, dissolved in 35 mL of CH_3CN , and reprecipitated with 100 mL of diethyl ether. Yield of $\text{MV}^{2+}\text{PF}_6^-$, 0.77 g (60% based on MVCl_2). The assay of $\text{MV}^{2+}\text{PF}_6^-$ was carried out spectrophotometrically as follows. The cation radical salt was transferred to a tared 10-mL volumetric flask that was capped and removed from the inert atmosphere box. After weighing, the volumetric flask was reintroduced into the drybox and solutions ($\sim 4\text{--}9 \times 10^{-5}$ M) of $\text{MV}^{2+}\text{PF}_6^-$ were prepared with acetonitrile that was degassed beforehand by four freeze-pump-thaw cycles. The standard solutions were transferred to a calibrated thin-layer cell (nominal pathlength 1.0 mm), removed from the drybox, and used to determine the extinction coefficients in Table I. Single crystals of $\text{MV}^{2+}\text{PF}_6^-$ suitable for X-ray crystallography were prepared directly for the deep purple precipitate obtained from aqueous solution after drying in vacuo for 5 h. The free-flowing air-sensitive powder (ca. 2.5 g) was dissolved in 25 mL of CH_3CN under an atmosphere of argon to afford a deep royal blue solution that was filtered through a bed of Celite to remove possible residual solids. The deep blue solution contained in a 250-mL Schlenk flask was carefully overlayered with approximately 100 mL of diethyl ether, and the two-phase mixture was placed in a freezer (-25°C). After 24 h, purple crystals of $\text{MV}^{2+}\text{PF}_6^-$ precipitated, and the pale blue supernatant was removed with the aid of a stainless-steel cannula. The crystals of $\text{MV}^{2+}\text{PF}_6^-$ were washed with diethyl ether (20 mL) and dried in vacuo.

Methylviologen Neutral (MV^0). The synthesis of MV^0 was based on a modification of the procedure by Carey and co-workers.¹² An aqueous solution of MVCl_2 (4.17 g, 16.2 mmol) in 70 mL of degassed water was reduced with sodium dithionite (2.82 g, 16.2 mmol) and aqueous ammonia (30 mL of a 10% solution) as described above. Sodium hydroxide (5 mL of a 2% aqueous solution) was added incrementally at 20-min intervals with the aid of a hypodermic syringe. Initially, the solution was deep purple-black and homogeneous, but after an hour of stirring, shiny dark red crystals could be observed on the walls of the flask. After 2 h, the supernatant had faded to a light brown color, and no additional crystals were observed. The crystals were collected by filtration in an atmosphere of argon and recrystallized from toluene/hexane at -25°C . Yield of MV^0 , 2.5 g (83% based on MVCl_2). IR (toluene, cm^{-1}): 1662 (s), 1353 (m), 1222 (s), 1195 (s), 1010 (s), 770 (m) (lit. 1665 (s), 1575 (w), 1355 (m), 1225 (s), 1195 (s), 1010 (s), 775 (m)). ^1H NMR (C_6D_6): δ 5.51 (d, $J = 6.5$ Hz, 2 H), 5.28 (d, $J = 7.1$ Hz, 2 H), 2.09 (s, 3 H). Crystals of MV^0 suitable for X-ray crystallography were grown by vapor-phase diffusion as follows: MV^0 (ca. 25 mg) was dissolved in 1 mL of toluene in an N_2 -filled inert atmosphere box. The solution was

carefully transferred to a 5-mL vial which was placed in an Erlenmeyer flask containing 10 mL of hexane. The flask was cooled in a freezer at -25°C and allowed to stand for 48 h. Deep red crystals of MV^0 were washed with hexane and dried in a stream of N_2 .

Instrumentation. Electronic spectra were recorded on a Hewlett-Packard 8450-A diode-array UV-vis spectrophotometer. The diffuse reflectance spectra were recorded on a Perkin-Elmer 330 UV-vis spectrometer equipped with a Hitachi 210-2101 integrating sphere. An alumina disk was used as reference for the diffuse-reflectance spectral measurements. IR spectra were recorded on a Nicolet 10DX FT spectrometer (2-cm^{-1} resolution) in either 1.0-mm NaCl cells or in KBr disks. NMR spectra were recorded on a JEOL FX 90Q spectrometer operating at 89.55 MHz. ESR spectra were recorded in sealed Pyrex tubes on a Varian E-110 spectrometer calibrated with DPPH. The highly air sensitive crystalline $\text{MV}^{2+}\text{PF}_6^-$ and MV^0 were stored and handled in a Vacuum Atmospheres HE 43-2 inert atmosphere box equipped with a Dri-Train inert-gas recirculator to maintain <5 ppm oxygen. Cyclic voltammetry was performed with an IR-compensated potentiostat driven by a Princeton Applied Research Model 175 Universal Programmer as described earlier.⁶⁰ Cyclic voltammograms were plotted on a Houston Instruments Model 2000 X-Y recorder (for scan rates <1.0 V s^{-1}) or displayed on a Tektronix 5115 storage oscilloscope (for scan rates between 1.0 and 200 V s^{-1}). Ferrocene was used as the reference standard in Table II.

Cyclic Voltammetry of Methylviologen and Its Reduced Forms. Electrochemical measurements of MV^0 , $\text{MV}^{2+}\text{PF}_6^-$, and $\text{MV}^{2+}(\text{PF}_6^-)_2$ were carried out in either dichloromethane or acetonitrile. The supporting electrolyte, tetra-*n*-butylammonium perchlorate (TBAP, G. F. Smith) was recrystallized from ethyl acetate and dried at room temperature in vacuo. The CV cell was equipped with Teflon valves and viton O-rings to ensure an air- and grease-free anolyte.⁶⁰ Solutions of $\text{MV}^{2+}\text{PF}_6^-$ and MV^0 were prepared in the drybox, whereas solutions of $\text{MV}^{2+}(\text{PF}_6^-)_2$ were prepared with standard Schlenk techniques.

X-ray Crystallography of the Reduced Forms of Methylviologen MV^0 and $\text{MV}^{2+}\text{PF}_6^-$. A dark red fragment of MV^0 having approximate dimensions $0.52 \times 0.24 \times 0.15$ mm was cut from a large prismatic slab and mounted in a random orientation of a Nicolet R3m/V automatic diffractometer. The sample was coated with a thin layer of epoxy owing to its air sensitivity. The radiation used was Mo $K\alpha$ monochromatized by a highly ordered graphite crystal. Final cell constants, as well as other information pertinent to data collection and refinement, were space group, $P2_1/c$, monoclinic; cell constants, $a = 14.449$ (5) Å; $b = 5.953$ (2) Å; $c = 13.542$ (5) Å; $\beta = 115.96$ (3) $^\circ$; $V = 1047$ Å³; molecular formula, $\text{C}_{12}\text{H}_{14}\text{N}_2$; formula weight, 186.28; formula units per cell, $Z = 4$; density, $\rho = 1.18$ g cm^{-3} ; absorption coefficient, $\mu = 0.66$ cm^{-1} ; radiation (Mo $K\alpha$), $\lambda = 0.71073$ Å; collection range, $4 < 2\theta < 50^\circ$; scan width, $\Delta\theta = 1.20 + (K\alpha_2 - K\alpha_1)^\circ$; scan speed range, 2.0 to 15.0 deg min^{-1} ; total data collected, 1831; independent data, $I > 2.5\sigma(I)$, 924; total variables, 135; $R = \sum||F_o| - |F_c|| / \sum|F_o|$, 0.052; $R_w = [\sum w(|F_o| - |F_c|)^2 / \sum w|F_o|^2]^{1/2}$, 0.034; weights, $w = \sigma(F)^{-2}$. The Laue symmetry was determined to be $2/m$, and from the systematic absences noted the space group was shown unambiguously to be $P2_1/c$. Intensities were measured using the ω scan technique, with the scan rate depending on the count obtained in rapid prescans of each reflection. Two standard reflections were monitored after every 2 h or every 100 data collected, and these showed no significant variation. In reducing the data, Lorentz and polarization corrections were applied; however, no correction for absorption was made due to the small absorption coefficient. The structure was solved by the SHELXTL direct methods program, which revealed the positions of all the non-hydrogen atoms in the asymmetric unit, consisting of two half-molecules situated about inversion centers. The usual sequence of isotropic and anisotropic refinement was followed, after which all hydrogens were entered in ideal calculated positions and constrained to riding motion, with a single variable isotropic temperature factor for the ring hydrogens and a single nonvariable one for the methyl hydrogens. The methyl groups were treated as ideal rigid bodies and allowed

(59) Luong, J. C.; Nadjio, L.; Wrighton, M. S. *J. Am. Chem. Soc.* **1978**, *100*, 5790.

(60) Kuchynka, D. J.; Kochi, J. K. *Inorg. Chem.* **1988**, *27*, 2574.

Table VIII. Atomic Coordinates ($\times 10^4$) and Equivalent Isotropic Displacement Parameters ($\text{\AA}^2 \times 10^3$)

	<i>x</i>	<i>y</i>	<i>z</i>	<i>U</i> (eq) ^a
MV ⁰				
N(1)	8727 (3)	2171 (6)	1529 (3)	64 (2)
N(2)	6327 (3)	4323 (7)	7902 (3)	69 (2)
C(1)	9511 (3)	3313 (7)	1434 (3)	60 (2)
C(2)	9999 (3)	2562 (7)	869 (3)	58 (2)
C(3)	9755 (3)	408 (7)	293 (3)	51 (2)
C(4)	8928 (3)	-715 (7)	421 (3)	62 (2)
C(5)	8458 (3)	112 (8)	1000 (3)	65 (2)
C(6)	8211 (4)	3022 (8)	2158 (4)	84 (3)
C(7)	5720 (3)	2632 (8)	7232 (4)	66 (2)
C(8)	5218 (3)	2847 (7)	6147 (4)	62 (2)
C(9)	5268 (3)	4870 (7)	5557 (3)	54 (2)
C(10)	5944 (3)	6550 (7)	6302 (4)	63 (2)
C(11)	6424 (3)	6248 (8)	7383 (4)	67 (3)
C(12)	6926 (3)	3979 (9)	9074 (3)	85 (3)
MV ⁺ PF ₆ ⁻				
P	851 (2)	1466 (2)	2100	56 (1)
F(1)	1316 (6)	670 (5)	1877 (25)	232 (2)
F(2)	-260 (5)	1095 (4)	2070 (22)	117 (1)
F(3)	424 (9)	2266 (5)	2370 (25)	284 (2)
F(4)	1944 (6)	1833 (6)	1955 (23)	179 (2)
F(5)	951 (9)	1297 (8)	4400 (15)	149 (2)
F(6)	671 (10)	1646 (7)	-104 (17)	154 (2)
N(1)	7681 (6)	444 (6)	7001 (21)	57 (2)
C(1)	7347 (9)	-309 (6)	7011 (23)	59 (2)
C(2)	6324 (7)	-514 (6)	6930 (21)	47 (2)
C(3)	5536 (7)	85 (6)	7200 (22)	41 (2)
C(4)	5932 (7)	879 (6)	7288 (21)	47 (2)
C(5)	6953 (8)	1034 (6)	7219 (22)	57 (2)
C(6)	8820 (8)	641 (7)	7099 (25)	144 (2)
N(2)	1765 (6)	3396 (4)	7041 (21)	49 (1)
C(7)	697 (7)	3271 (6)	7205 (24)	57 (2)
C(8)	31 (7)	3892 (5)	7038 (23)	47 (2)
C(9)	370 (7)	4678 (5)	7187 (23)	40 (2)
C(10)	1456 (7)	4773 (5)	7250 (22)	41 (2)
C(11)	2122 (7)	4167 (5)	7277 (22)	42 (2)
C(12)	2508 (7)	2730 (6)	7433 (23)	71 (2)

^a Equivalent isotropic *U* defined as one-third of the trace of the orthogonalized U_{ij} tensor.

to rotate freely. After all shift/esd ratios were less than 0.2, convergence was reached at the agreement factors listed above. No unusually high correlations were noted between any of the variables in the last cycle of full-matrix least-squares refinement, and the final difference density map showed a maximum peak of about 0.2 e \AA^{-3} . All calculations were made using Nicolet's SHELXTL PLUS (1987) series of crystallographic programs to yield the final atomic coordinates listed in Table VIII. The molecular structure of MV⁰ was solved as two crystallographically independent molecules with distances and angles (Table III) that were identical within experimental error. Each molecule possessed overall D_{2h} symmetry with a mean deviation from planarity of 0.009 and 0.002 Å. Each structure showed marked bond alternation of localized single and double bonds. The slight lengthening of the central C-C bond [e.g., compare C1-C2 (1.32 Å) relative to C3-C3' (1.36 Å)] may be a consequence of resonance effects as indicated in the related dithiopyranilidene.²⁸ The molecules do not form a stack but pack instead in a herringbone pattern similar to that found in simple aromatic hydrocarbons.³⁸

A large, dark purple multifaceted wedge of MV⁺PF₆⁻ having approximate dimensions $0.40 \times 0.35 \times 0.20 \text{ mm}$ was coated with epoxy and mounted as described above. The crystallographic data were space group, *Pnn2*, orthorhombic; cell constants, $a = 12.773$ (3) Å; $b = 16.902$ (5) Å; $c = 6.578$ (2) Å; $V = 1420 \text{ \AA}^3$; molecular formula, $\text{C}_{12}\text{H}_{14}\text{N}_2^{+}\text{PF}_6^{-}$; formula weight, 331.25; formula units per cell, $Z = 4$; density, $\rho = 1.55 \text{ g cm}^{-3}$; absorption coefficient, $\mu = 2.47 \text{ cm}^{-1}$; radiation (Mo $K\alpha$), $\lambda = 0.71073 \text{ \AA}$; collection range,

$4^\circ < 2\theta < 50^\circ$; scan width, $\Delta\theta = 1.4 + (K\alpha_2 - K\alpha_1)^\circ$; scan speed range, 2.0–15.0 deg min⁻¹; total data collected, 1485; independent data, $I > 3\sigma(I)$, 718; total variables, 190; $R = \sum||F_o| - |F_c|| / \sum|F_o|$, 0.064; $R_w = [\sum w(|F_o| - |F_c|)^2 / \sum w|F_o|^2]^{1/2}$, 0.047; weights, $w = \sigma(F)^{-2}$. The Laue symmetry was determined to be *mmm*, and from the systematic absences noted the space group was shown to be either *Pnn2* or *Pnnm*. Intensities were measured using the ω scan technique, with the scan rate depending on the count obtained in rapid prescans of each reflection. Two standard reflections were monitored after every 2 h or every 100 data collected, and these showed only a 3% decay over the course of the experiment. In reducing the data, Lorentz and polarization corrections were applied as described above. In the noncentrosymmetric *Pnn2* space group, difference maps phased on the Patterson solution produced an acceptable model. Some difficulty was encountered, since there were two independent half-molecules of the cation in the asymmetric unit, each positioned about a 2-fold axis. Both of these molecules were almost planar (vide infra) and were situated at essentially the same height along the *c* axis. Four of the six fluorines were also at the same height. Such a concentration of electron density in one plane, with fairly large gaps between planes, accounted for the relatively lower percentage of observed data which was obtained from such a large sample crystal. All hydrogens were added at ideal positions and constrained to riding motion, with a single variable isotropic temperature factor for the phenyl hydrogens and a nonvariable one for the methyl hydrogens. All non-hydrogen atoms were refined anisotropically. No attempt was made to determine the sense of direction in this polar, nonenantiomorphous space group. After all shift/esd ratios were less than 0.5, convergence was reached at the agreement factors listed above. No unusually high correlations were noted between any of the variables in the last cycle of full-matrix least squares refinement, and the final difference density map showed a maximum peak of about 0.3 e \AA^{-3} . Calculations were made using the Nicolet programs described above to yield the final atomic coordinates listed in Table VIII. The crystal contained two independent MV⁺ moieties designated as MVI and MVII, both with overall C_2 symmetry arising from a distorted chair geometry in each half. MVI was characterized by an interannular torsional angle of 6° and a displacement of the ring nitrogen from the mean plane (fitted to C1, C2, C4, and C5) of 0.16 Å. The corresponding torsional angle and nitrogen displacement for MVII was 11° and 0.08 Å. The ring-ring bond distance was considerably shorter for MVII than for MVI (1.40 vs 1.44 Å). The two cations alternated in an infinite stack parallel to the *c* axis. The rings of the cations did not lie directly over each other, but were displaced by an angle of 37° with a ring-ring distance (measured from the midpoint of the C-C interannular bond) of 3.29 Å.

Bulk Magnetic Susceptibility of MV⁺PF₆⁻. Magnetic susceptibility measurements were performed on a Johnson-Matthey JME magnetic susceptibility balance calibrated with HgCo(SCN)₄.⁶¹ The tared susceptibility cell was introduced into the inert-atmosphere box, loaded with recrystallized MV⁺PF₆⁻ (~20 mg) and capped with a rubber septum. The sample was removed from the drybox and reweighed, and its molar susceptibility was determined as $\chi_M = -1.6 \times 10^{-4} \text{ cgs units mol}^{-1}$. The correction for the diamagnetic susceptibility of the closed-shell electrons⁶² gave a corrected susceptibility of $\chi_M^{\text{corr}} = -1.0 \times 10^{-5} \text{ cgs units mol}^{-1}$, that indicated minimal residual diamagnetism.

Acknowledgment. We thank J. D. Korp for crystallographic assistance and the National Science Foundation, Texas Advanced Research Program, and the Robert A. Welch Foundation for financial support.

(61) Angelici, R. J. *Synthesis and Technique in Inorganic Chemistry*; Saunders: Philadelphia, 1969.

(62) Jolly, W. L. *The Synthesis and Characterization of Inorganic Compounds*; Prentice-Hall: Englewood Cliffs, NJ, 1970.